

pubs.acs.org/macroletters Letter

Cross-Linked Polyolefins through Tandem ROMP/Hydrogenation

Caitlin S. Sample, Brenden D. Hoehn, and Marc A. Hillmyer*



Cite This: ACS Macro Lett. 2024, 13, 395–400



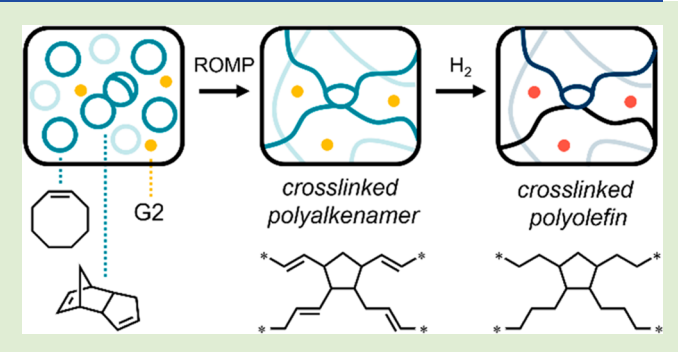
ACCESS I

III Metrics & More

Article Recommendations

Supporting Information

ABSTRACT: Cross-linked polyolefins have important advantages over their thermoplastic analogues, particularly improved impact strength and abrasion resistance, as well as increased chemical and thermal stability; however, most strategies for their production involve postpolymerization cross-linking of polyolefin chains. Here, a tandem ring-opening metathesis polymerization (ROMP)/hydrogenation approach is presented. Cyclooctene (COE)-codicyclopentadiene (DCPD) networks are first synthesized using ROMP, after which the dispersed Ru metathesis catalyst is activated for hydrogenation through the addition of hydrogen gas. The reaction temperature for hydrogenation must be sufficiently high to allow mobility within the system, as dictated by thermal



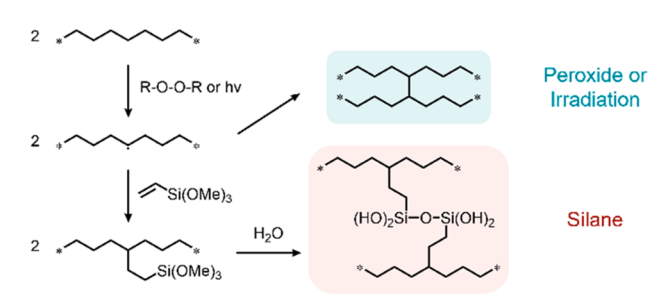
transitions (i.e., glass and melting transitions) of the polymeric matrix. COE-rich materials exhibit branched-polyethylene-like crystallinity (25% crystallinity) and melting points ($T_{\rm m}$ = 107 °C), as well as excellent ductility (>750% extension), while majority DCPD materials are glassy ($T_{\rm g}$ = 84 °C) and much stiffer (E = 710 MPa); all materials exhibit high tensile toughness. Importantly, hydrogenation of olefins in these cross-linked materials leads to notable improvements in oxidative stability, as saturated networks do not experience the same substantial degradation of mechanical performance as their unsaturated counterparts upon prolonged exposure to air.

hile polyethylene (PE) accounts for over a third of the plastic market, limitations in its mechanical properties and thermal/chemical stability prevent its implementation in high performance applications. One strategy to circumvent this is to introduce interchain cross-links, which can be achieved by peroxide-initiated or irradiation-induced radical cross-linking or incorporation of silanes that subsequently hydrolyze and condense (Scheme 1a). The benefits imbued by cross-linking, increased impact, abrasion, stress cracking, thermal, and chemical resistances,² have enabled applications in biomedicine (e.g., artificial joints),³ construction (e.g., plumbing),⁴ and electronics (e.g., cable coatings). However, each cross-linking strategy comes with drawbacks, whether it is the relatively large quantities of peroxides required and their associated byproducts⁶ or the inconsistencies in the cross-linking distribution from moisture diffusion (e.g., in silane chemistry, crosslinks concentrated in surface and amorphous regions)^{7,8} or solid-state processing (e.g., in irradiation processes, cross-links concentrated in amorphous regions).9

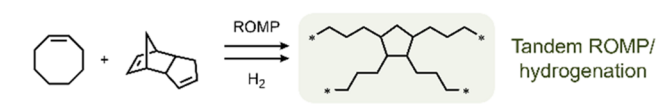
An alternate route toward hydrocarbon-based thermosets is through ring-opening metathesis polymerization (ROMP) of bicyclic olefins, particularly dicyclopentadiene (DCPD). Polydicyclopentadiene (PDCPD) exhibits attractive mechanical properties, including high impact resistance and heat deflection temperature, that can further be tuned through the introduction of monocyclic comonomers. Additionally, the ability to incorporate cleavable moieties provides promising

Scheme 1. (a) Conventional and (b) Proposed Synthetic Strategies toward Cross-Linked Polyolefins

(a) Conventional



(b) Proposed



Received: February 19, 2024 Revised: March 7, 2024 Accepted: March 13, 2024 Published: March 19, 2024





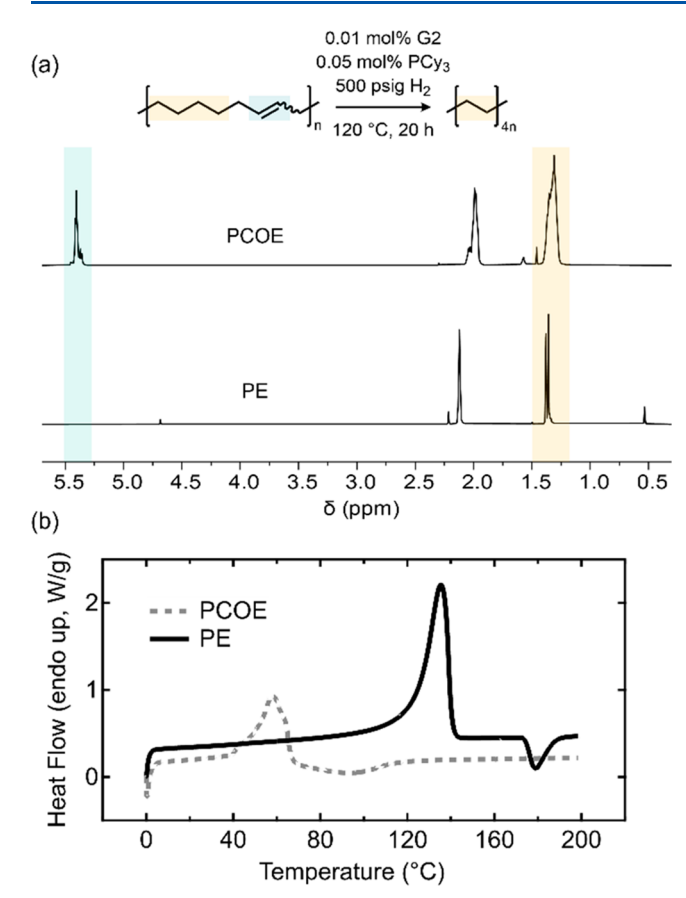


Figure 1. (a) ¹H NMR spectra of a representative PCOE and PE and (b) DSC traces for linear polymers before (PCOE) and after (PE) hydrogenation.

avenues for preventing waste accumulation. 15-17 However, PDCPD undergoes rapid surface oxidation due to the high concentration of unsaturated olefins, and side reactions at these sites can lead to a dramatic decrease in mechanical performance that greatly shortens the lifetime of PDCPDbased parts. 18 While hydrogenation can be used to mitigate this degradation in analogous linear ROMP polymers, 19,20° the network structure of cross-linked PDCPD presents an obstacle toward chemistries that require solvation of the polymer substrate. Whereas linear PDCPD can be hydrogenated through traditional strategies, 21,22 the only reported hydrogenation of PDCPD networks has been in the preparation of aerogels, in which loosely cross-linked DCPD gels were swollen with a reactive solution for chemical hydrogenation.²³ While this hydrogenation did indeed improve the oxidative stability of the resultant materials, the multiple solvent exchange steps required are not practical at scale or for a diverse range of systems.

Inspired by previous work using tandem catalysis to generate linear polyolefins, ^{24–27} as well as investigations into the hydrogenation of bulk polymers, ^{28,29} we hypothesized that the Ru metathesis catalyst used in the ROMP of cross-linked polyalkenamers, and therefore dispersed within the network, would undergo a transformation to a hydrogenation catalyst upon exposure to H₂, thereby affording homogeneous hydrogenation of the network olefins (Scheme 1b). The monomers selected to give polyolefin materials for this study were *cis*-cyclooctene (COE) and DCPD, with COE-rich networks expected to give PE-like properties, while DCPD-

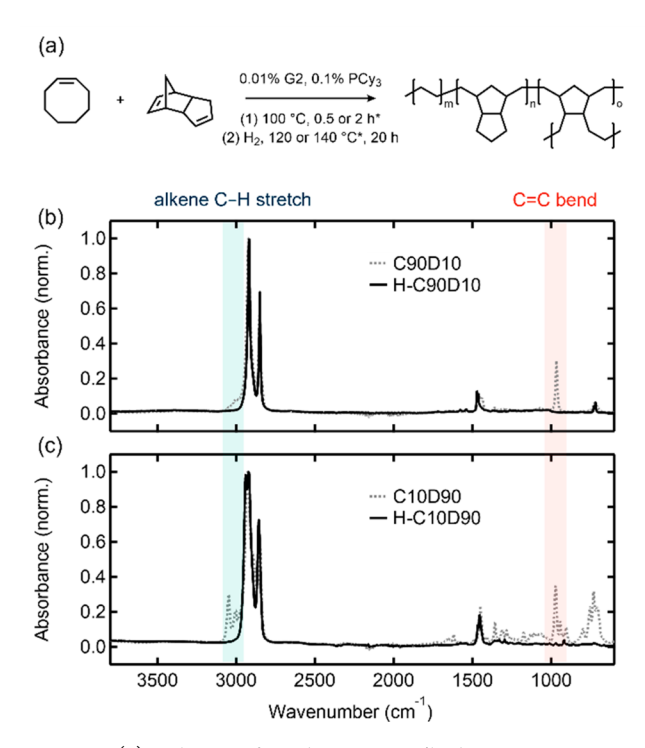


Figure 2. (a) Scheme of tandem ROMP/hydrogenation reaction. *Numbers represent conditions for C90D10 and C10D90, respectively. FTIR spectra of (a) C90D10 and H-C90D10 and (b) C10D90 and H-C10D90. Peaks corresponding to alkene C—H stretching and C=C bending are highlighted.

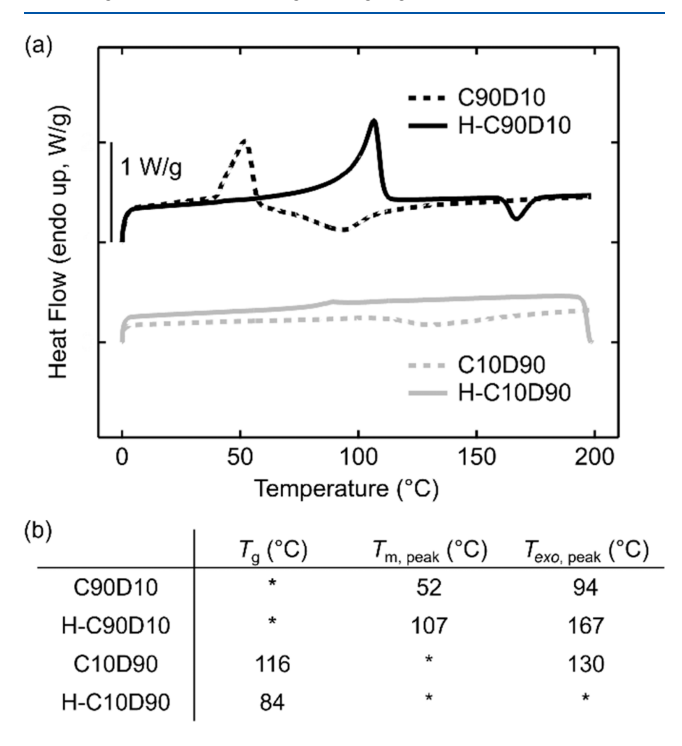


Figure 3. DSC traces of C90D10, H–C90D10, C10D90, and H–C10D90, measured under air. First heating curve (heating rate 10 $^{\circ}$ C/min) is shown. C90D10 and H–C90D10 shifted vertically by 1 W/g. (b) Table of $T_{\rm g}$, $T_{\rm m}$, peak, and $T_{\rm exo,peak}$ (peak temperature of signal attributed to oxidative exotherm) values. *Feature not observed in measured temperature range.

rich networks would enable exploration of the properties of hydrogenated PDCPD.

(a)	C90D10	H-C90D10	C10D90	H-C10D90
E (MPa)	2.0 ± 0.27	62 ± 1.7	650 ± 22	710 ± 36
$rac{arepsilon_{ ext{yield}}}{(\%)}$	160 ± 6.4	24 ± 1.4	7.2 ± 0.68	8.2 ± 0.70
$\sigma_{ m yield}$ (MPa)	1.0 ± 0.067	5.8 ± 0.55	46 ± 2.4	50. ± 2.0
$\mathcal{E}_{break} \ (\%)$	760 ± 190	760 ± 47*	240 ± 7.3	250 ± 28
$\sigma_{ extsf{break}}$ (MPa)	2.4 ± 1.4	18 ± 2.9*	47 ± 0.86	54 ± 4.7
U_{T} (MJ m ⁻³)	12 ± 4.2	97 ± 11*	87 ± 3.8	98 ± 17

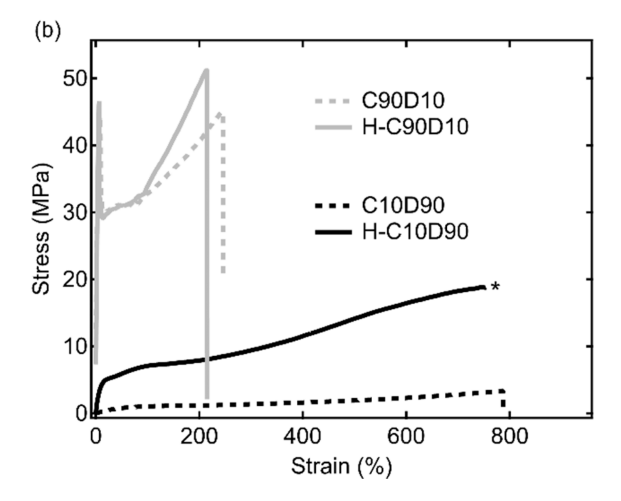


Figure 4. (a) Mechanical properties of samples before and after hydrogenation. Values are average ± standard deviation for 5 (C90D10, C10D90, H–C10D90) or 3 (H–C90D10) replicates. (b) Representative tensile curves for C90D190, H–C90D190, C10D90, and H–C10D90. *Samples pulled out from grips.

As an initial study, varied amounts of COE and DCPD were mixed and 0.01 mol % Grubbs second generation catalyst (G2) was added in minimal quantities of toluene (1.5 vol %). However, rapid gelation limited the pot life and handling time, a known challenge in the synthesis of DCPD-based materials.³⁰ Inhibitors can be added to delay this gelation, and PCy3 was investigated due to its combined inhibitory effect³¹ and promotion of subsequent hydrogenation.²⁶ Dynamic mechanical analysis was used to assess pot life at varied [PCy₃]:[G2] ratios for a model system of 50 mol % COE and 50 mol % DCPD (Figure S1), and 10 equiv of PCy₃ relative to G2 was found to give a working time of ~10 min. Subsequent ³¹P NMR characterization revealed that the PCy3 used had oxidized to POCy₃ (Figure S2).³² While the exact time frame of this oxidation is unknown, samples prepared over the course of this study showed both reliable inhibition and consistent hydrogenation results. Select hydrogenation results for other inhibitors studied are presented in the Supporting Information (Figure S3).

To test the hypothesis that tandem ROMP/hydrogenation could be successful in a bulk monomer/polymer context, conditions for pure COE were explored with the temperature of hydrogenation varied from 40 to 120 $^{\circ}$ C (Figure S4). The dependence of the extent of hydrogenation on reaction temperature (from 33% at 40 $^{\circ}$ C to >99.9% at 120 $^{\circ}$ C) over

a fixed time suggests a relationship to the melting transitions of PCOE (\sim 55 °C) and linear PE (\sim 130 °C). As these materials contain almost no solvent, mobility within the system is dominated by polymer chain dynamics. While the amorphous domains are mobile due to the low glass transition temperatures of both PCOE and PE, the semicrystalline nature of both polymers likely impacts facile diffusion of the catalyst and H₂, as well as limiting access to the backbone olefins (i.e., in crystallites). The multimodal melting transitions of partially hydrogenated PCOE suggest multiple domains with varied crystalline character, with the highest peak melting temperature of 120 °C approaching that of linear PE (Figure S5). Importantly, as the hydrogenation temperature approached the melting transition of PE ($T_{\rm hydrogenation} = 120$ °C), nearly quantitative (>99.9%) saturation of the backbone was realized (Figure 1).

Building on these results, two monomer compositions were selected for further investigation: 90 mol % COE/10 mol % DCPD (PE-like, labeled C90D10) and 10 mol % COE/90 mol % DCPD (PDCPD-like, labeled C10D90) (Figure 2a). The former was found to be the minimal loading of DCPD to give a high degree of cross-linking, as determined by gel fractions of >90% (Figure S6), while the latter was the maximum loading of DCPD that still produced a liquid solution that was easy to handle prior to ROMP. For C90D10, curing at 100 $^{\circ}\text{C}$ for 2 h was required to reach high gel fractions (>90%), while the C10D90 sample with 90% DCPD reached gel fractions of >95% within 30 min at 100 °C. Subsequent exposure to 500 psig H₂ provided conditions for hydrogenation; however, as with pure PCOE, the thermal transitions dictated the necessary reaction temperature. Due to its similarity with PCOE, C90D10 is fully hydrogenated to H-C90D10 at 120 °C, as reflected in the Fourier-transform infrared (FTIR) spectra by the complete disappearance of the peaks associated with the olefin C—H stretch and C=C bend (Figure 2b). While the DCPD loading of C10D90 suppresses crystallinity, its higher T_{σ} requires an increase in the reaction temperature to 140 °C to yield the fully hydrogenated H-C10D90 (Figure 2c); temperatures below that lead to surface hydrogenation but an unsaturated interior (Figure S7).

As expected, hydrogenation affects the thermal properties of the resultant networks, which were characterized by differential scanning calorimetry (DSC, Figure 3). Both C90D10 and H-C90D10 exhibit semicrystalline character, with a peak melting temperature increasing from 52 °C, typical for PCOE, to 107 °C, typical of branched PE, upon hydrogenation. Likewise, hydrogenation led to increase in crystallinity from 16% to 24% (calculated using reference enthalpies of melting of 230³³ and 309 J/g^{34} for perfectly crystalline PCOE and PE, respectively). In addition to thermal transitions, an exotherm was observed for samples heated in an air environment, which we hypothesize is due to oxidation reactions. The peak temperature of this exotherm shifted from 94 to 167 °C after hydrogenation in the C90D10/H-C90D10 samples, evidence of an increase in oxidative stability. For the predominantly DCPD-based system, a decrease in T_g from 115 °C (C10D90) to 84 °C (H-C10D90) is observed, similar to the decrease in $T_{\rm g}$ measured in hydrogenated PDCPD aerogels.²³ Notably, the $T_{\rm g}$ feature was followed by an exotherm in C10D90, likely due to the increased mobility of the network enabling the diffusion of oxygen throughout the system; the disappearance of this feature under a nitrogen atmosphere supports its attribution to oxidation (Figure S8). In contrast, no such exotherm is

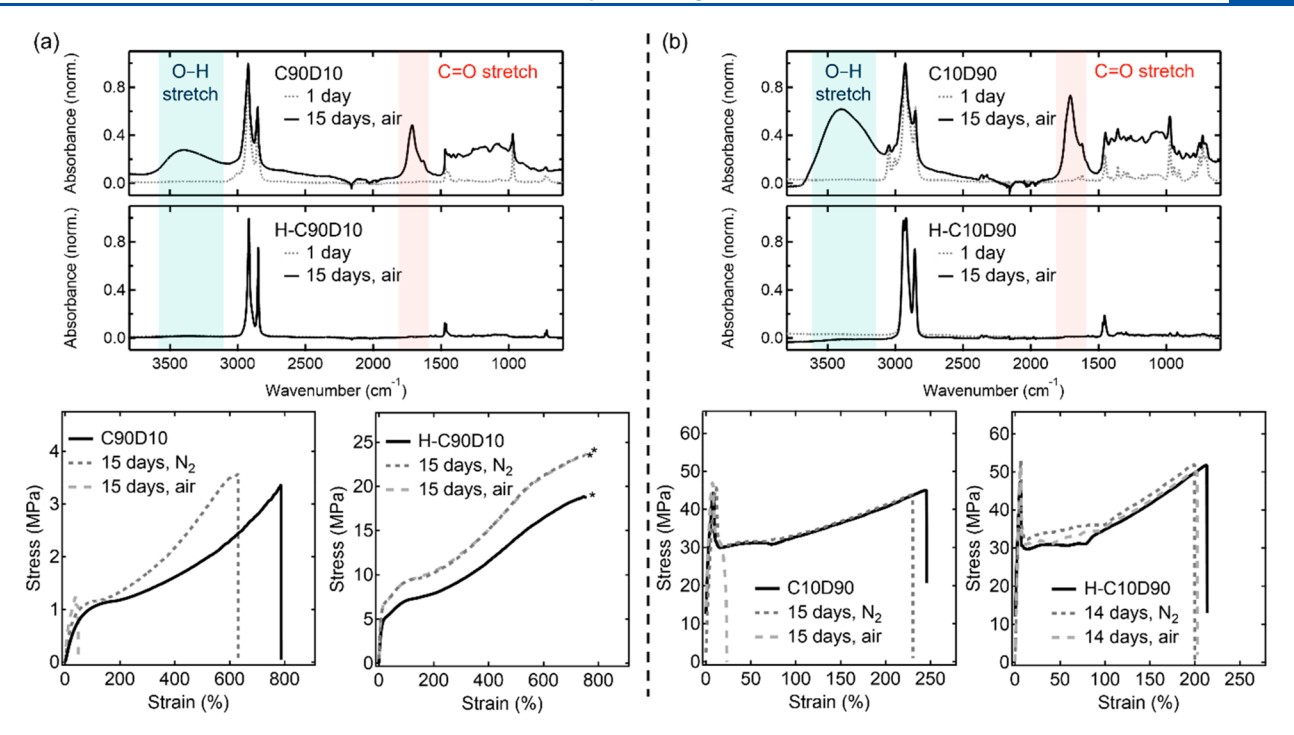


Figure 5. FTIR spectra and representative tensile curves of (a) C90D10 and H–C90D10 and (b) C10D90 and H–C10D90. FTIR taken within 1 day of synthesis and after 15 days of air exposure. Peaks corresponding to O—H and C=O stretching are highlighted. Tensile tests taken within 3 days of synthesis (stored under N_2) and after 15 days of air or N_2 exposure (except for H–C10D90, which was measured at 14 days). *Samples pulled out from grips.

observed for H–C10D90 within the entire temperature window probed, which gives further evidence of hydrogenation providing important benefits for the stability of these highly cross-linked materials.

To understand how hydrogenation influences mechanical performance, 3-5 replicate samples for each formulation were subjected to tensile testing (Figure 4, images in Figure S9, and full stress-strain plots in Figure S10). H-C90D10 proved challenging to test, as samples consistently pulled from grips before failure, despite employing a variety of preventative strategies. As such, curves for these samples (Figures 3b and S10a) are plotted to the point where the sample came out of the grips. Regardless, much of the difference in behavior of these materials compared to their nonhydrogenated counterparts is still evident. The PCOE-like C90D10 is relatively soft (E = 1.5 MPa) and ductile, with ultimate extensions ~750%. Upon hydrogenation, H-C90D10 retains the ductility while becoming substantially stiffer (E = 62 MPa), likely due to the enhanced crystallinity (24% vs 16% before hydrogenation). Furthermore, H-C90D10 exhibits a double yield, characteristic of polyethylene,³⁵ followed by marked strain stiffening. DSC measurements taken before and after testing indicate that crystallinity increases post elongation (from 25% to 27%, Figure S11). In contrast, C10D90 and H-C10D90 show minimal differences in tensile behavior as a consequence of hydrogenation. After an initial sharp yield into necking, these materials exhibit surprising ductility for highly cross-linked, glassy materials, and this, combined with the high strength, results in notable tensile toughness values of 87 and 98 MJ m⁻³, respectively.

Based on the differences in oxidative stability observed via thermal characterization, the evolution in chemical and mechanical properties of these materials was also assessed. Samples were characterized by FTIR spectroscopy within 1 day of synthesis and underwent tensile testing at 3 days (to minimize variation from any early physical aging effects). Two equivalent sets of samples were exposed to either a nitrogen or air atmosphere at 18-20 °C for 14-15 days, during which period notable yellowing was observed for the nonhydrogenated samples, but not their hydrogenated counterparts (Figure S12). Samples were further characterized via FTIR spectroscopy and tensile testing (Figures 5 and S13 and Table S1). The difference in chemical changes between the nonhydrogenated and hydrogenated samples after air exposure is apparent in the FTIR spectra, with the former showing the emergence of numerous new peaks (particularly those associated with O—H and C=O stretching)²³ and the latter showing negligible change. These chemical differences have a dramatic correlation to the mechanical properties of these materials. For the majority COE samples stored under N2, an increase in stiffness is likely due to physical aging effects such as densification and further crystallization. However, the behavior of those same materials stored under air depends on their olefinic character, with C90D10 becoming very brittle and H-C90D10 showing little variation between storage conditions. The highly cross-linked nature of the predominantly DCPD samples limits aging when stored under N2, but when stored in air, the nonhydrogenated C10D90 became brittle, while H-C10D90 maintained its ductility.

The results presented here have important implications for the ROMP-based synthesis of new materials. By leveraging the existing catalyst within metathesis-derived polymer networks, material properties can be substantially changed via the in situ hydrogenation of as-synthesized polymers. Careful selection of conditions above the key thermal transitions of the material enabled sufficient mobility to allow for networks to be fully hydrogenated. This transformation is catalytic in nature, without the need for solvent or a hydrogen precursor source,

and thus aligned with key principles of green chemistry. With the COE/DCPD monomer system explored herein, materials akin to cross-linked polyethylene or to PDCPD were easily accessed, and it is expected that intermediate compositions would broaden the range of possible properties. We envision that this approach could be further extended to other ROMP systems, including those containing degradable comonomers for more sustainable end-of-life targets.

ASSOCIATED CONTENT

Data Availability Statement

The primary data underlying this study are openly available in The Data Repository for University of Minnesota (DRUM) at https://doi.org/10.13020/s2rv-1918.

Supporting Information

The Supporting Information is available free of charge at https://pubs.acs.org/doi/10.1021/acsmacrolett.4c00108.

Experimental details, sample images, NMR and FTIR spectra, tensile testing and gel fraction data, and DMA and DSC traces (PDF)

AUTHOR INFORMATION

Corresponding Author

Authors

Caitlin S. Sample – Department of Chemistry, University of Minnesota, Minneapolis, Minnesota 55455-0431, United States; orcid.org/0000-0002-8622-0180

Brenden D. Hoehn – Department of Chemical Engineering and Materials Science, University of Minnesota, Minneapolis, Minnesota 55455-0431, United States

Complete contact information is available at: https://pubs.acs.org/10.1021/acsmacrolett.4c00108

Author Contributions

C.S.S. and M.A.H. conceived the project and designed the experimental approach. C.S.S. and B.D.H. carried out the experiments described. All authors contributed to data analysis and preparation of the manuscript.

Notes

The authors declare no competing financial interest.

ACKNOWLEDGMENTS

This work was supported by the National Science Foundation (Award No. DMR-2003454). NMR experiments were performed on instruments supported by the Office of the Vice President of Research, College of Science and Engineering, the Department of Chemistry at the University of Minnesota, and the Office of the Director, National Institutes of Health of the National Institutes of Health (Award No. S10OD011952). FTIR measurements were carried out in the Characterization Facility, University of Minnesota, which receives partial support from the NSF through the MRSEC (Award Number DMR-2011401) and the NNCI (Award Number ECCS-2025124) programs. The content is solely the responsibility of the authors and does not necessarily represent the official views of the National Institutes of Health. The authors would like to acknowledge Dr. Thomas Smith, Dr.

Letitia Yao, Dr. David Giles, Dr. Asheesh Shukla, and Dr. Bing Luo for their assistance with characterization. We would also like to thank Dr. Yoon-Jung Jang, Dr. Elizabeth Feinberg, and Daniel Krajovic, and Dr. Mara Kuenen for their helpful discussions and insight.

REFERENCES

- (1) Geyer, R.; Jambeck, J. R.; Law, K. L. Production, Use, and Fate of All Plastics Ever Made. *Sci. Adv.* **2017**, *3*, e1700782.
- (2) Ahmad, H.; Rodrigue, D. Crosslinked Polyethylene: A Review on the Crosslinking Techniques, Manufacturing Methods, Applications, and Recycling. *Polym. Sci. Eng.* **2022**, *62*, 2376–2401.
- (3) Zhang, H.; Guo, Y.; Tian, F.; Qiao, Y.; Tang, Z.; Zhu, C.; Xu, J. Discussion of Orientation and Performance of Crosslinked Ultrahigh-Molecular-Weight Polyethylene Used for Artificial Joints. *ACS Appl. Mater. Interfaces* **2022**, *14*, 29230–29237.
- (4) Hiles, M.; Grossutti, M.; Dutcher, J. R. Classifying Formulations of Crosslinked Polyethylene Pipe by Applying Machine-Learning Concepts to Infrared Spectra. *J. Polym. Sci., Part B: Polym. Phys.* **2019**, 57, 1255–1262.
- (5) Hedir, A.; Moudoud, M.; Lamrous, O.; Rondot, S.; Jbara, O.; Dony, P. Ultraviolet Radiation Aging Impact on Physicochemical Properties of Crosslinked Polyethylene Cable Insulation. *J. Appl. Polym. Sci.* **2020**, *137*, 48575.
- (6) Sahyoun, J.; Crepet, A.; Gouanve, F.; Keromnes, L.; Espuche, E. Diffusion Mechanism of Byproducts Resulting from the Peroxide Crosslinking of Polyethylene. *J. Appl. Polym. Sci.* **2017**, *134*, 44525.
- (7) Shieh, Y.-T.; Liau, J.-S.; Chen, T.-K. An Investigation of Water Crosslinking Reactions of Silane-Grafted LDPE. *J. Appl. Polym. Sci.* **2001**, *81*, 186–196.
- (8) Oliveira, G. L.; Costa, M. F. Optimization of Process Conditions, Characterization and Mechanical Properties of Silane Crosslinked High-Density Polyethylene. *Mater. Sci. Eng., A* **2010**, 527, 4593–4599.
- (9) Forster, A. L.; Tsinas, Z.; Al-Sheikhly, M. Effect of Irradiation and Detection of Long-Lived Polyenyl Radicals in Highly Crystalline Ultra-High Molar Mass Polyethylene (UHMMPE) Fibers. *Polymers* (Basel) 2019, 11, 924.
- (10) Davidson, T. A.; Wagener, K. B.; Priddy, D. B. Polymerization of Dicyclopentadiene: A Tale of Two Mechanisms. *Macromolecules* **1996**, 29, 786–788.
- (11) Rule, J. D.; Moore, J. S. ROMP Reactivity of *Endo-* and *Exo*-Dicyclopentadiene. *Macromolecules* **2002**, *35*, 7878–7882.
- (12) Autenrieth, B.; Jeong, H.; Forrest, W. P.; Axtell, J. C.; Ota, A.; Lehr, T.; Buchmeiser, M. R.; Schrock, R. R. Stereospecific Ring-Opening Metathesis Polymerization (ROMP) of *Endo*-Dicyclopentadiene by Molybdenum and Tungsten Catalysis. *Macromolecules* **2015**, 48, 2480–2492.
- (13) Chen, J.; Burns, F. P.; Moffitt, M. G.; Wulff, J. E. Thermally Crosslinked Functionalized Polydicyclopentadiene with a High $T_{\rm g}$ and Tunable Surface Energy. *ACS Omega* **2016**, *1*, 532–540.
- (14) Dean, L. M.; Wu, Q.; Alshangiti, O.; Moore, J. S.; Sottos, N. R. Rapid Synthesis of Elastomers and Thermosets with Tunable Thermomechanical Properties. ACS Macro Lett. 2020, 9, 819–824.
- (15) Ivanoff, D. G.; Sung, J.; Butikofer, S. M.; Moore, J. S.; Sottos, N. R. Cross-Linking Agents for Enhanced Performance of Thermosets Prepared via Frontal Ring-Opening Metathesis Polymerization. *Macromolecules* **2020**, *53*, 8360–8366.
- (16) Shieh, P.; Zhang, W.; Husted, K. E. L.; Kristufek, S. L.; Xiong, B.; Lundberg, D. J.; Lem, J.; Veysset, D.; Sun, Y.; Nelson, K. A.; Plata, D. L.; Johnson, J. A. Cleavable Comonomers Enable Degradable, Recyclable Thermoset Plastics. *Nature* **2020**, 583, 542–547.
- (17) Davydovich, O.; Paul, J. E.; Feist, J. D.; Aw, J. E.; Bonner, F. J. B.; Lessard, J. J.; Tawfick, S.; Xia, Y.; Sottos, N. R.; Moore, J. S. Frontal Polymerization of Dihydrofuran Comonomer Facilitates Thermoset Deconstruction. *Chem. Mater.* **2022**, *34*, 8790–8797.
- (18) David, A.; Huang, J.; Richaud, E.; Yves Le Gac, P. Impact of Thermal Oxidation on Mechanical Behavior of Polydicylopentadiene:

- Case of Non-Diffusion Limited Oxidation. *Polym. Degrad. Stab.* **2020**, 179, No. 109294.
- (19) Otsuki, T.; Goto, K.; Komiya, Z. Development of Hydrogenated Ring-Opening Metathesis Polymer. J. Polym. Sci. Part A Polym. Chem. 2000, 38, 4661–4668.
- (20) Lee, L.-B. W.; Register, R. A. Hydrogenated Ring-Opened Polynorbornene: A Highly Crystalline Atactic Polymer. *Macromolecules* **2005**, 38, 1216–1222.
- (21) Kodemura, J.; Natsuume, T. Synthesis and Properties of Hydrogenated Ring-Opening Polymers of Endo/Exo-Dicyclopenta-diene. *Polym. J.* **1995**, *27*, 1167–1172.
- (22) Hayano, S.; Takeyama, Y.; Tsunogae, Y.; Igarashi, I. Hydrogenated Ring-Opened Poly(*Endo*-Dicyclopentadiene)s Made via Stereoselective ROMP Catalyzed by Tungsten Complexes: Crystalline Tactic Polymers and Amorphous Atactic Polymer. *Macromolecules* **2006**, *39*, 4663–4670.
- (23) Lenhardt, J. M.; Kim, S. H.; Nelson, A. J.; Singhal, P.; Baumann, T. F.; Satcher, J. H. Increasing the Oxidative Stability of Poly (Dicyclopentadiene) Aerogels by Hydrogenation. *Polymer* **2013**, 54 (2), 542–547.
- (24) Bielawski, C. W.; Louie, J.; Grubbs, R. H. Tandem Catalysis: Three Mechanistically Distinct Reactions from a Single Ruthenium Complex. J. Am. Chem. Soc. 2000, 122, 12872–12873.
- (25) Drouin, S. D.; Zamanian, F.; Fogg, D. E. Multiple Tandem Catalysis: Facile Cycling between Hydrogenation and Metathesis Chemistry. *Organometallics* **2001**, *20*, 5495–5497.
- (26) Camm, K. D.; Castro, N. M.; Liu, Y.; Czechura, P.; Snelgrove, J. L.; Fogg, D. E. Tandem ROMP—Hydrogenation with a Third-Generation Grubbs Catalyst. *J. Am. Chem. Soc.* **2007**, *129*, 4168—4169.
- (27) Sample, C. S.; Kellstedt, E. A.; Hillmyer, M. A. Tandem ROMP/Hydrogenation Approach to Hydroxy-Telechelic Linear Polyethylene. *ACS Macro Lett.* **2022**, *11*, 608–614.
- (28) Gilliom, L. R. Catalytic Hydrogenation of Polymers in the Bulk. *Macromolecules* **1989**, 22, 662–665.
- (29) Gilliom, L. R.; Honnell, K. G. Observation of a Reaction Front in the Bulk Catalytic Hydrogenation of a Polyolefin. *Macromolecules* **1992**, 25, 6066–6068.
- (30) Robertson, I. D.; Dean, L. M.; Rudebusch, G. E.; Sottos, N. R.; White, S. R.; Moore, J. S. Alkyl Phosphite Inhibitors for Frontal Ring-Opening Metathesis Polymerization Greatly Increase Pot Life. *ACS Macro Lett.* **2017**, *6*, 609–612.
- (31) P'Pool, S. J.; Schanz, H.-J. Reversible Inhibition/Activation of Olefin Metathesis: A Kinetic Investigation of ROMP and RCM Reactions with Grubbs' Catalyst. *J. Am. Chem. Soc.* **2007**, *129*, 14200–14212.
- (32) Caraballo, R.; Rahm, M.; Vongvilai, P.; Brinck, T.; Ramström, O. Phosphine-Catalyzed Disulfide Metathesis. *Chem. Commun.* **2008**, 6603–6605.
- (33) Schneider, W. A.; Müller, M. F. Crystallinity of Trans-Polyoctenamer: Characterization and Influence of Sample History. *J. Mol. Catal.* **1988**, *46*, 395–403.
- (34) Richardson, M. J. Precision Differential Calorimetry and the Heat of Fusion of Polyethylene. *J. Polym. Sci. Part C Polym. Symp.* **1972**, 38, 251–259.
- (35) Brooks, N. W.; Duckett, R. A.; Ward, I. M. Investigation into Double Yield Points in Polyethylene. *Polymer* **1992**, *33*, 1872–1880.